JOURNAL OF GEOPHYSICAL RESEARCH, VOL. 105, NO. D17, PAGES 22,299–22,309, SEPTEMBER 16, 2000

Tropical stratospheric gravity wave activity and relationships to clouds

M. Joan Alexander
Northwest Research Associates, Colorado Research Associates division, Boulder

Jadwiga H. Beres
University of Washington, Seattle

Leonhard Pfister
NASA Ames Research Center, Moffett Field, California

Abstract. Wind measurements from NASA's ER-2 aircraft in the stratosphere are used to obtain information on the momentum flux carried by gravity waves with horizontal wavelengths between 5 and 150 km. Tropical data are compared with the cloud brightness temperature below the aircraft as an indicator of deep convective activity. A striking correlation between cold, high clouds and large gravity wave momentum flux is seen in data from the Stratosphere-Troposphere Exchange Project (STEP) tropical campaign during the monsoon season over northern Australia and Indonesia. There is an enhancement in the flux carried by waves propagating against the background wind in these observations. The same analysis was performed with data from more recent ER-2 flights over the tropical Pacific Ocean during the Airborne Southern Hemisphere Ozone Experiment/Measurements for Assessing the Effects of Stratospheric Aircraft (ASHOE/MAESA), Stratospheric Tracers of Atmospheric Transport (STRAT), and Photochemistry of Ozone Loss in the Arctic Region in Summer (POLARIS) campaigns which took place in 1994, 1995-1996, and 1997, respectively. These data also show a correlation between gravity wave momentum flux and deep convective clouds, but the relationship is much weaker, and the magnitudes of the momentum flux over the deepest clouds are about 7 times smaller than those seen in the STEP data. The reasons for these differences remain uncertain, but possibilities include both real geophysical differences and differences associated with the flight paths during the 1987 versus later campaigns.

1. Introduction

Gravity waves are an important mechanism for vertical momentum and energy transport in the atmosphere, and they drive large-scale circulation patterns at upper levels where they break or are otherwise dissipated. They exist in the atmosphere with a wide range of horizontal and vertical scales, frequencies, and phase speeds. These properties, as well as when and where they appear, have been observed to vary with geographic location, season, and time of day. Although gravity waves are important to the momentum budgets in global circulation models (GCM), these scales of waves are generally too small to be modeled directly in GCMs, and their effects must be parameterized as momentum forcing and diffusive mixing terms. Their effects in the atmosphere are highly dependent on both the characteristic properties of the waves and the quantity of momentum flux they carry [e.g., *Lindzen and Holton*, 1968; *Lindzen*, 1981].

Convection is believed to be an important source of gravity waves, particularly in the tropics and at higher latitudes in summertime, where high phase speed waves are expected to drive important circulation patterns in the stratosphere and mesosphere. The quasi-biennial oscillation (QBO) in the lower stratosphere, the semi-annual oscillations (SAO) at both the stratopause and mesopause, and the meridional transport circulation in the middle atmosphere are all believed to be driven at least in part by momentum flux dissipation associated with high phase speed gravity waves [*Holton*, 1983; *Dunkerton*, 1982; 1997; *Alexander and Rosenlof*, 1996; *Ray et al.*, 1998]. Very little is known about the properties and occurrence of these high phase speed waves because they will tend to have long vertical wave-

Paper number 2000JD900326.
0148-0227/00/2000JD900326$09.00

lengths and high frequencies and are therefore difficult to observe with traditional profiling techniques with radiosondes and rockets. These techniques require the removal of a background profile in order to examine the gravity wave perturbations, and long vertical wavelength waves are difficult to distinguish from mean state and planetary-scale wave variations unless the data are collected at fine time resolution.

Mesoscale models of deep convection show generation of a broad spectrum of gravity waves when the models include a deep stratospheric layer above the cloud [*Fovell et al.*, 1992; *Alexander et al.*, 1995; *Alexander and Holton*, 1997; *Piani et al.*, 2000]. In these simulations of squall line convection, the waves generated display a broad spectrum of horizontal wavelengths and intrinsic frequencies; however, their vertical wavelengths tend to be closely associated with the depth of the latent heating in the strong central updraft behind and above the gust front [*Alexander et al.*, 1995; *Pandya and Alexander*, 1999]. The waves that appear most directly above this deep central heating region have the highest intrinsic frequencies and shortest horizontal wavelengths. Lower frequencies and longer horizontal wavelengths create a fan-like pattern above the storm. This pattern in the wave intrinsic frequencies is expected above a central compact wave source region because the slope of a wave's ray path above the horizontal is the ratio of the vertical to horizontal components of the group velocity (c_{gx}, c_{gz}):

$$\left(\frac{dz}{dx}\right)_{ray} = \frac{c_{gz}}{c_{gx}} = \left|\frac{k}{m}\right| = \left(\frac{\hat{\omega}^2 - f^2}{N^2 - \hat{\omega}^2}\right)^{1/2}. \quad (1)$$

Ray paths follow lines of constant phase. In (1), k and m are the horizontal and vertical wavenumbers, respectively; $\hat{\omega}$ is the intrinsic frequency; N is the buoyancy frequency, f is the Coriolis parameter, and it has been assumed that $m >> (2H)^{-1}$. For waves with a common m, those with larger k (smaller horizontal wavelength) will display steeper slopes and will appear more directly above the source, as will waves with higher $\hat{\omega}$.

The short horizontal wavelength, high-frequency waves above deep convection can carry significant momentum flux. *Alexander and Pfister* [1995] demonstrated how vertical flux of horizontal momentum carried by these waves can be estimated from in situ wind, temperature, and pressure measured from stratospheric aircraft. In a case study from the Stratosphere-Troposphere Exchange Project (STEP) campaign over Darwin, Australia, in 1987, large momentum fluxes, comparable to those that appeared in the mesoscale simulations, were observed from the ER-2 aircraft in the stratosphere above a very deep storm. The momentum flux was large along the flight path directly above the storm, and it fell to very small values once the aircraft left the vicinity of the deepest part of the storm cloud. Similar close associations between deep convection and gravity wave activity have been observed elsewhere [*Röttger*, 1980; *Larsen et al.*, 1982; *Pfister et al.*, 1986, 1993a, b; *Sato et al.*, 1995; *Dewan et al.*, 1998; *McLandress et al.*, 2000].

In the present paper, we examine a large collection of in situ wind measurements from the ER-2 aircraft during flights over tropical convection and examine the statistical relationship between the momentum flux carried by gravity waves in the stratosphere and the depth of the convection below the aircraft. Section 2 describes the observations and the analysis method, section 3 is a discussion of these results, and section 4 is a summary with conclusions.

2. Stratospheric Aircraft Data and Analysis

2.1. Gravity Wave Momentum Flux

The Meteorological Measurement System (MMS) flown on NASA's ER-2 aircraft makes in situ measurements of all three components of the wind velocity along the flight path as well as temperature and pressure [*Scott et al.*, 1990]. From the vector wind measurements, we can extract information on the vertical flux of horizontal momentum carried by gravity waves in the lower stratosphere. The vertical wind measurement is an important component of this analysis but is also a difficult measurement to make. Previous analyses have shown that these vertical winds can be sufficiently accurate to extract meaningful information on gravity waves [*Alexander and Pfister*, 1995]. The determination of vertical wind is, however, subject to several sources of error:

1. The algorithms used to extract the vertical wind cannot completely remove the effects of turning maneuvers and sharp changes in aircraft altitude that cause pressure fluctuations and erroneous vertical winds. We therefore use only data from straight and approximately level flight path segments in the present analysis.

2. The accuracy of the vertical wind measurements is better than 0.1 m s^{-1} (P. Bui, personal communication, 1999); however, the measurements can be subject to drift in the zero reference due to integrated errors in the accelerometer measurements along the flight path [*Scott et al.*, 1990]. This red noise can be significant when changes in the wind over distances much longer than 100 km are desired. We therefore restrict our attention to waves with wavelengths of less than 150 km.

3. The precision in the measurements is important for determining the amplitude of the wave perturbations that can be detected above noise levels. The precision in the vertical wind is 0.1 m s^{-1} (P. Bui, personal communication, 1999). The measurements are recorded at 1-Hz or better sampling, which translates to a horizontal distance traveled by the aircraft of approximately 200 m or less. We are mainly interested in gravity waves with horizontal wavelengths of the order of 10 km and longer because shorter-scale waves are much more easily trapped or reflected at low altitudes, and so they contribute little to the middle atmosphere momentum

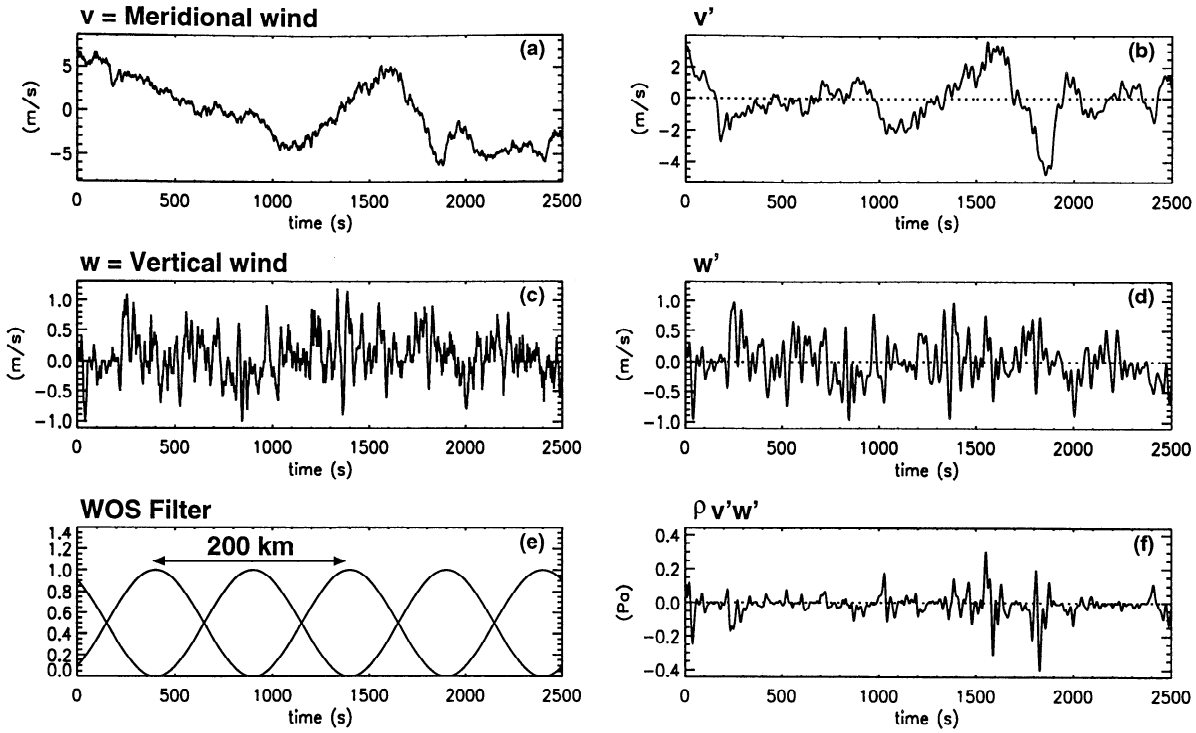

Figure 1. Example time series of observations from the ER-2 aircraft flying at 17.7-km altitude on January 22, 1987. (a) Meridional wind and (b) perturbations for waves with wavelengths of $\sim 5-150$ km. (c) Vertical wind and (d) perturbations for waves with wavelengths of $\sim 5-150$ km. (e) Illustration of the size and shape of the weighting functions applied in the WOS filtering process. (f) North-south component of the momentum flux.

budget. The random error for our gravity wave analysis can therefore be reduced substantially through averaging of adjacent measurements or low-pass filtering without loss of information.

To estimate momentum flux along the flight path, the components of the wind are Fourier analyzed by using a weighted overlapping segment (WOS) technique [*Percival and Walden*, 1993]. A Hanning (cosine) taper function is applied sequentially along the flight path to segments of the time series 1000 s long (see Figure 1). The aircraft cruises at $\sim$200 m s^{-1}; so 1000 s of data represents $\sim$200 km of distance. The gravity wave periods will generally be longer than the time it takes the plane to fly through a full cycle of the wave. The time along the flight path is therefore best thought of as a distance flown through an approximately stationary wave pattern, and the fast Fourier transform (FFT) of the time series is a better measure of the horizontal wavenumber spectrum than the gravity wave frequency spectrum.

The FFT of the tapered data segment is computed after removal of the horizontal wind linear trend and the vertical wind mean value over the segment interval. The transform is then low-pass filtered to remove the smallest-scale fluctuations with a tapered filter. The filter leaves 40-s periods ($\sim$8-km wavelengths) and longer unattenuated and completely removes 15-s periods ($\sim$2.5-km wavelengths) and shorter. The result is then transformed back to real space. Each adjacent data segment overlaps with the previous one by 50%, and the results from each segment are added together creating a continuous time series of wind fluctuations $(u'(t), v'(t), w'(t))$ for the zonal, meridional, and vertical components of the wind vector (Figure 1) representing waves with wavelengths roughly in the range 5–150 km. The products $\bar{\rho}(u'w', v'w')$ contain information on the vertical flux of zonal and meridional momentum, respectively, for waves of this scale; $\bar{\rho}$ represents the background atmospheric density along the flight path which is determined from the measured temperature and pressure. An example of this procedure is shown in Figure 1. The overlapping taper functions sum to unity except at the very edges of the time series, where some of the first and last 500 s ($\sim$100 km) of tapered data are not recovered. *Alexander and Pfister* [1995] compared results similar to these to $\bar{\rho}(u'w')$ computed in the stratosphere above a storm cloud in a numerical simulation.

The pseudomomentum flux for a monochromatic wave with intrinsic frequency $\hat{\omega}$ much larger than the Coriolis parameter f is the wavelength-averaged covariance $\bar{\rho}(\overline{u'w'}, \overline{v'w'})$. (For lower-frequency waves, a correction factor $(1 - f^2/\hat{\omega}^2)$ should be included [*Fritts and Vincent*, 1987].) Our momentum flux estimates contain information not on a single-wavelength wave, but on the band of wavelengths of $\sim$5–150 km. The results described later will be magnitudes of $\bar{\rho}(u'w', v'w')$ binned

according to geophysical parameters along the flight path such as cloud height. This binning accomplishes the same sort of wavelength averaging needed to estimate the momentum flux $\bar{\rho}(\overline{u'w'}, \overline{v'w'})$, but without presuming the wavelength a priori. The binned values will be referred to simply as momentum fluxes in the results that follow.

2.2. Cloud Top Temperature From a Narrow Field-of-View Infrared Radiometer

During the 1987 STEP Tropical campaign [*Russell et al.*, 1993], the ER-2 carried a down-looking narrow field-of-view infrared radiometer [*Liou et al.*, 1990] that measured cloud top temperature in two channels along the flight path. The radiance and brightness temperatures were reported at 0.5-Hz sampling. We will use the brightness temperature T_b in the 10.5-μm channel as an indicator of cloud top temperature (approximately inversely proportional to cloud top height) below the aircraft. The time series of T_b and corresponding magnitude $\bar{\rho}|v'w'|$ of the time series in Figure 1f is shown in Figure 2. Note that the largest values occur over the coldest, highest clouds in this example. This will be shown to be a common occurrence in what follows.

2.3. Correlations Between Gravity Wave Momentum Flux and Cloud Top Temperature During the STEP Tropical Campaign

The STEP campaign included many flights of the ER-2 aircraft at upper tropospheric and lower stratospheric altitudes directly over the very deep convective storms that occurred over northern Australia and Indonesia during January and February 1987. This time of year is known as the monsoon season. Values of the magnitude of momentum flux M are computed along the flight paths as

$$M = \bar{\rho}(|u'w'|^2 + |v'w'|^2)^{1/2}. \quad (2)$$

Data from all of the available stratospheric flight segments are then binned according to the T_b below the aircraft in 20 K bin intervals. The result is shown in Figure 3. The data for times when the aircraft was flying over land and ocean have been binned separately because over land, topographically generated waves and variations in surface heating caused by cloud patchiness can in some cases obscure the correlation. The oceanic measurements show a very clear linear anticorrelation between M and T_b for $T_b > 230$ K. The largest values of M occur above the coldest highest clouds $T_b = 200-240$ K. These results include data from flights 5, 6, 8, 9, 10, 12, 13, and 14 (see *Russell et al.* [1993] for flight details). Other flights could not be used either because the navigation system failed or no cloud data were obtained. *Russell et al.* [1993] show maps of the flight paths overlain on cloud satellite imagery for reference.

Cloud top temperatures less than 235 K have been used as a high-cloud threshold in statistical studies of convection [*Chen et al.*, 1996] and global rainfall correlations [*Arkin and Meisner*, 1987]. Such deep convection is associated with heavy rainfall and deep regions of latent heating that appear as the centers of gravity wave forcing in the mesoscale convection models [*Fovell et al.*, 1992; *Alexander et al.*, 1995; *Alexander and Holton*, 1997; *Piani et al.*, 2000]. In these simulations, the waves that appear most directly over the cloud have high intrinsic frequencies and carry significant momentum flux vertically into the middle atmosphere. The momentum flux magnitudes in Figure 3 are very significant. For example, such waves could provide a substantial fraction of the momentum flux needed to drive the quasi-biennial oscillation (QBO) observed in stratospheric winds [*Alexander and Holton*, 1997; *Piani et al.*, 2000]. If the relationship in Figure 3a is representative of tropical convection in general, then we can combine this result with statistics on the occurrence of deep convection in the tropics [*Zhang*, 1993] to estimate

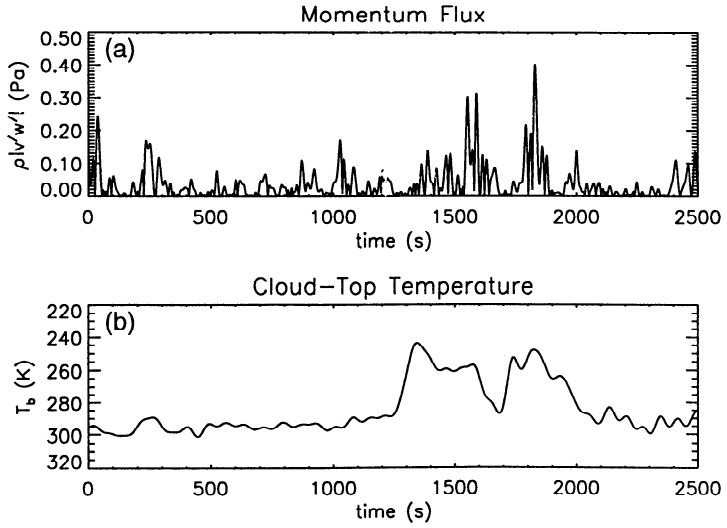

Figure 2. Time series for the same flight segment as in Figure 1. (a) Magnitude of the north-south momentum flux. (b) Brightness temperature of the cloud tops below the aircraft.

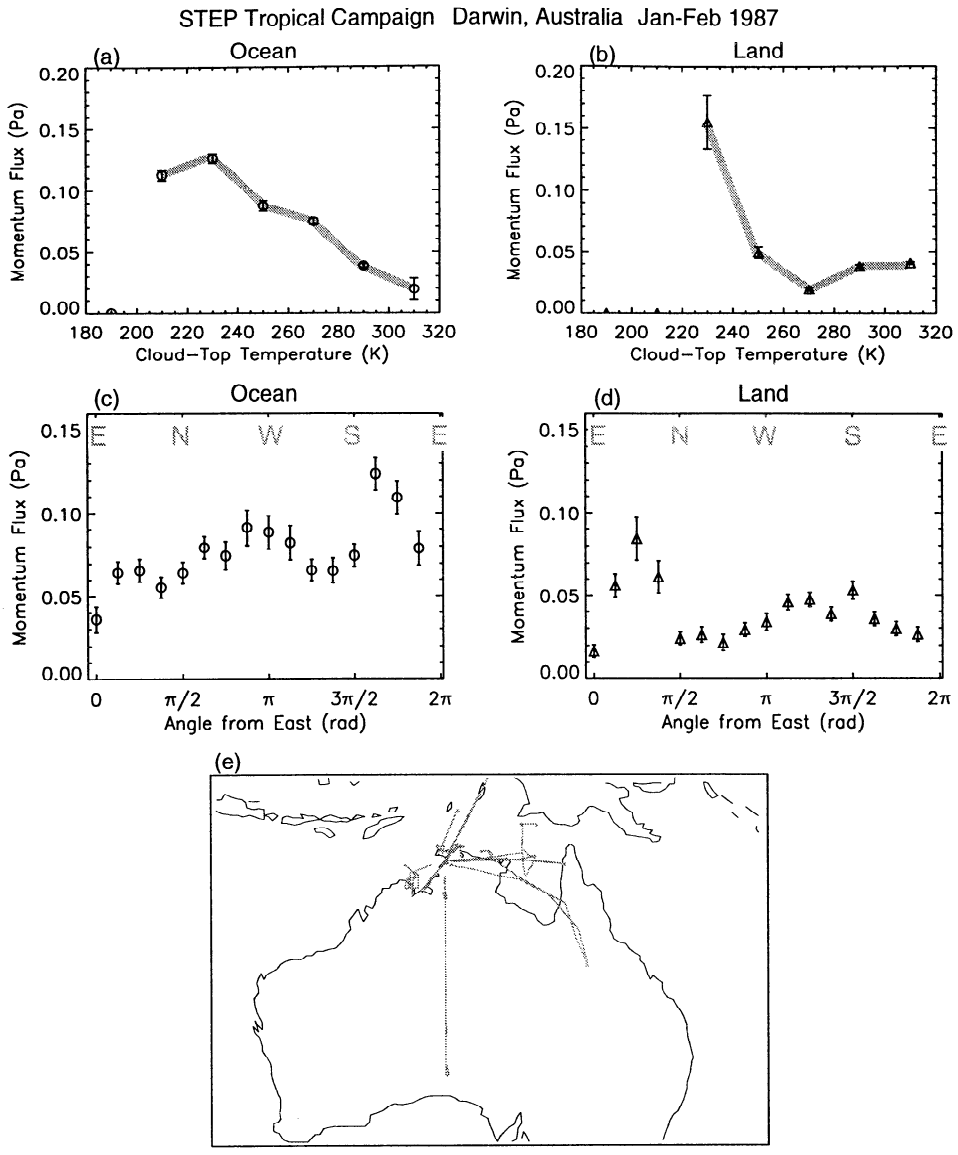

Figure 3. Momentum flux observations in the stratosphere binned according to the cloud top brightness temperature below the aircraft measured by the onboard infrared radiometer during the STEP Tropical campaign over (a) ocean and (b) land. Zero flux indicates that no data occurred in that temperature range. Momentum flux observations binned according to the direction of the flux over (c) ocean and (d) land. Error bars represent the standard error in the mean. (e) Light lines show flight paths superimposed on map contours for the Australia-Indonesia region.

the time- and area-averaged flux at tropical latitudes. *Zhang* [1993] estimates a mean fractional coverage of clouds with $T_b < 215$ K in the latitude band 20°N-20°S of $\sim 2\%$. This coverage times the momentum flux carried by waves above deep clouds during the STEP campaign would give an estimate of the time-averaged flux in the 20°N-20°S region of $\sim 2 \times 10^{-3}$ Pa, a value close to the total gravity wave momentum flux estimated as necessary to drive the QBO [*Dunkerton*, 1997].

Figures 3c and 3d show the distribution of momentum flux with propagation direction. Most of the flux is carried by southeastward propagating waves over ocean and northeastward over land. A bias toward eastward propagating gravity wave activity has also been observed by using radiosonde observations from this part of the world [*Hamilton and Vincent*, 1995; *Vincent and Alexander*, 2000], although those data primarily included only very low frequency waves, whereas we focus on higher-frequency waves in this study. Such anisotropies in the flux could greatly affect the role the waves play in driving middle atmosphere circulations. Note that the background wind at typical ER-2 flight levels was westward with eastward shear aloft (the westerly phase of the QBO) during the STEP campaign.

2.4. Gravity Wave Momentum Flux and Clouds From Other Tropical ER-2 Flights

Several other ER-2 observational campaigns included flights across tropical latitudes in the central Pacific. During the Stratospheric Tracers of Atmospheric Trans-

port (STRAT) campaign, four flights south from Hawaii (21°N) to just south of the equator were included to observe latitudinal variations in the mixing ratios of chemical species observed by instruments on the ER-2. A similar "south survey" flight was also conducted during the Photochemistry of Ozone Loss in the Arctic Region in Summer (POLARIS) mission. The Airborne Southern Hemisphere Ozone Experiment/Measurements for Assessing the Effects of Stratospheric Aircraft (ASHOE/MAESA) campaign included six survey and ferry flights over the tropical Pacific Ocean. The dates and locations of these flights are given in Table 1. These 11 flights are selected for analysis of the gravity wave momentum flux and the relationship to cloud properties below the aircraft as was done in the previous section for the STEP data.

No onboard radiometer measurements were made during these campaigns. Cloud properties below the ER-2 aircraft were instead estimated for each of these flights from infrared satellite imagery at 11 μm. For STRAT, cloud brightness temperatures were estimated from Advanced Very High Resolution Radiometer (AVHRR) images. For POLARIS, GOES Variable (GVAR) images were used. For ASHOE/MAESA, either GOES or GMS satellite images were used. These are nominally available at 0.5- to 3-hour time intervals and 4- to 10-km resolution.

Brightness temperature for the flight paths was determined from the satellite imagery by extracting T_b underneath the aircraft as a function of its latitude and longitude. This was done for the two satellite images that were taken closest to the time at which the airplane passed a given location. The final value was calculated by using a weighted time average of the two brightness temperatures.

Figure 4 shows the correlation between the 5- to 150-km gravity wave momentum flux and cloud top brightness temperature for the tropical Pacific ER-2 flights. Figures 4a–4c show correlations from individual campaigns, and Figure 4d shows the composite correlation for all 11 flights. On flights that overflew deep convective clouds, some relationship between deep convection and larger gravity wave momentum fluxes can be seen; however, the magnitudes of these fluxes are ~7 times smaller than those observed during the STEP campaign (Figure 3a), and the correlation slope is smaller. We discuss some of the possible reasons for the differences between Figures 3a and 4d in the next section.

We have not further examined the distribution of these fluxes with propagation direction as was done for the STEP data. The background atmospheric conditions for these various flights are more diverse, and the fluxes in the averages seen in Figure 4 are too small to warrant such an analysis. Instead such questions must be addressed via case studies for larger-amplitude events that will be the subject of future work.

3. Discussion

There are several differences between the STEP data (Figure 3a) and the tropical Pacific data (Figure 4d) that might explain the different relationships they give. They include differences in the type of cloud observations, differences related to the different nature of the convection in these two distinct geographical regions, and differences in the wind measurements between the STEP campaign in 1987 and the other campaigns which took place 1994–1997.

3.1. Cloud Data Differences

The STEP cloud observations come from radiometer measurements on board the ER-2 aircraft and are therefore coincident in space and time with the ER-2 in situ wind measurements. The later campaigns rely on satellite images which have poorer spatial resolution and are available only at time intervals up to several hours. Perhaps the one-to-one correspondence in space and time between the cloud and gravity wave observations is important to the correlation? To address this question, cloud top brightness temperature was estimated for the STEP flights from GMS satellite images just as was done for the STRAT, POLARIS, and ASHOE/MAESA

Table 1. Summary of Convection Associated With Intertropical Convergence Zone Flights

Campaign	Date	Flight Path	Convective Activity
ASHOE/MAESA	March 21, 1994	Hawaii south	high cirrus shield
ASHOE/MAESA	March 22, 1994	Hawaii south	over weak convection
ASHOE/MAESA	March 27, 1994	Hawaii to Guam	over weak convection
ASHOE/MAESA	Oct.24, 1994	Guam to Hawaii	edge of deep convection
ASHOE/MAESA	Oct.26, 1994	Hawaii south	none
ASHOE/MAESA	Oct.29, 1994	Hawaii south	edge of deep convection
STRAT	Nov.5, 1995	Hawaii south	over deep convection
STRAT	Aug.1, 1996	Hawaii south	edge of weak convection
STRAT	Aug.8, 1996	Hawaii south	edge of weak convection
STRAT	Dec.11, 1996	Hawaii south	little or none
POLARIS	Sept.23, 1997	Hawaii south	late stage deep convection

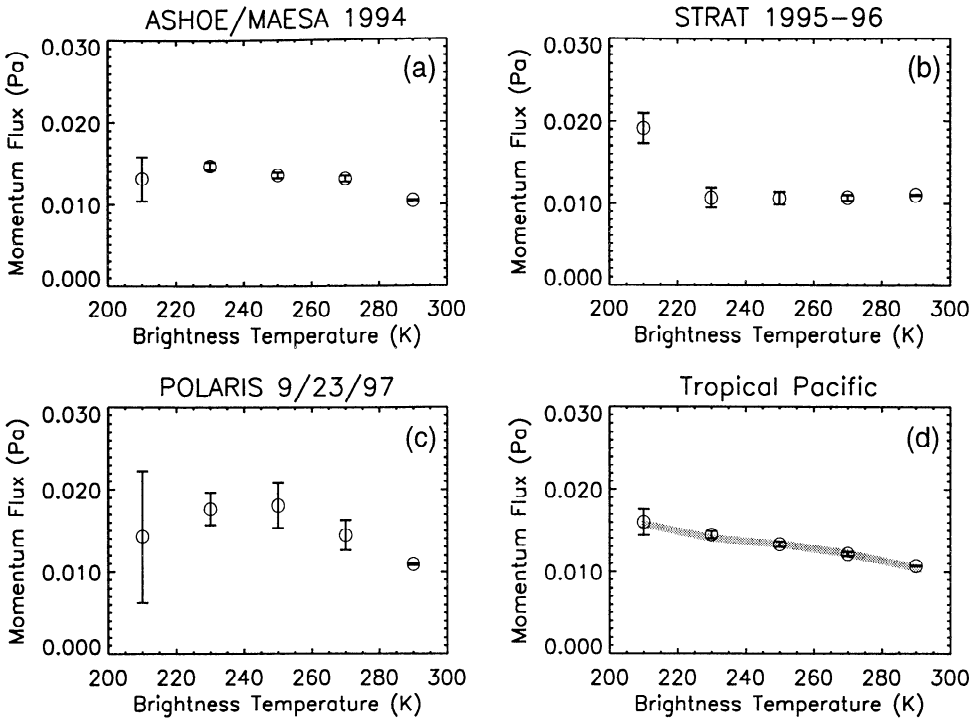

Figure 4. Momentum flux observations in the stratosphere binned according to the cloud top brightness temperature below the aircraft as measured by satellite for flights over the tropical Pacific Ocean. (a) ASHOE/MAESA campaign including six flights in March and October 1994. (b) STRAT campaign including four flights in November 1995 and August and December 1996. (c) POLARIS campaign flight on September 23, 1997. (d) Momentum flux versus cloud brightness temperature from all 11 flights combined.

flights. The correlation of these satellite-based brightness temperatures with gravity wave momentum flux for the STEP data is shown in Figure 5. A very similar correlation to that seen in Figure 3a is reproduced. Some differences are expected not only because of spatial and temporal resolution, but also because the STEP radiometer measurements are much more precisely calibrated. Some additional flight segments could also be used in creating Figure 5 because of different brightness temperature data coverage. The comparison suggests that the lower spatial and temporal resolution of the satellite cloud data compared with the radiometer observations is not a major factor in explaining the differences between the STEP results and those from the later campaigns over the tropical Pacific Ocean.

3.2. Changes in MMS Observations Between STEP 1987 and the 1994-1997 Campaigns

The meteorological measurements have also changed in the interval between the STEP campaign in 1987 and the more recent flights over the tropical Pacific.

The MMS determines wind by measuring the differential pressure among holes placed symmetrically around the aircraft nose. These pressure measurements as well

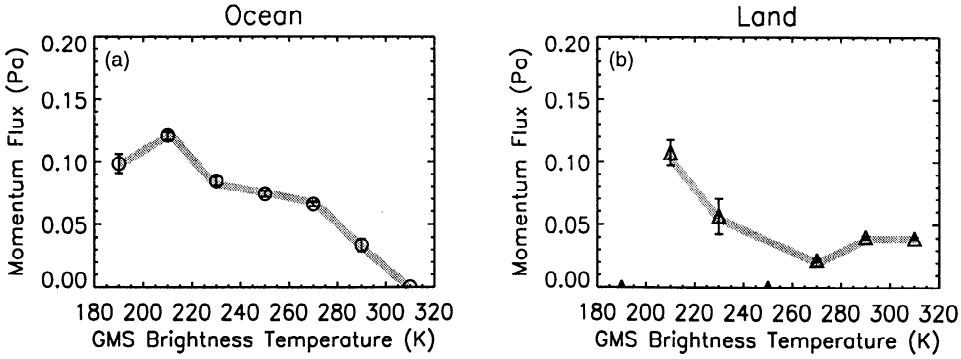

Figure 5. Same as Figures 3a and 3b but using GMS satellite observations of cloud top brightness temperature.

as temperature and static pressure measurements are used to infer the wind relative to the aircraft. Precise knowledge of the aircraft velocity then allows a subtraction to be made to infer the winds relative to the ground. The vertical wind in particular is a small value that is the difference between two very large terms and is therefore especially difficult to determine accurately [*Scott et al.*, 1990]. We have excluded wave scales of >150 km because of red noise errors. The vertical wind is particularly sensitive to them because, unlike horizontal wind variance which is red at all our scales of interest, the vertical wind variance has a flat spectral shape [*Bacmeister et al.*, 1996].

Some of the changes to the MMS have been improvements to the inertial navigation system that should only improve the wind measurements. Spectral studies of more recent data [*Bacmeister et al.*, 1996] compared with earlier data [*Murphy*, 1989] suggest that these improvements have reduced the white noise floor improving measurements of short horizontal scale ($\leq$2 km) fluctuations, but they have been excluded from our analysis. On the other hand, the ER-2 aircraft flew with a modified nose cone for the STRAT, POLARIS, and ASHOE flights. The new nose included a central hole used to intake air for special chemical measurements. This change in the nose shape changed the airflow around the nose and inadvertently reduced the sensitivity of the differential pressure measurements by about a factor of 2 (P. Bui and S. Bowen, personal communication, 1999). This reduced sensitivity would theoretically increase the errors in the determination of the angles of attack and sideslip of the air relative to the aircraft, lead to errors in the wind determination, and particularly affect the vertical wind at small values. The reduced sensitivity would not affect observations of large-amplitude waves as shown by *Chan et al.* [1993]. Our gravity wave momentum flux analysis depends on the vertical wind; so it could be subject to increased error at small vertical wind values. This could raise the level of the estimates at high T_b where no clouds are present, but cannot alone explain the reduced values at cold T_b in Figure 4d compared with Figure 3a. Therefore the reduced sensitivity associated with changes in the nose cone does not appear to explain the differences between the Australian and the tropical Pacific data.

3.3. Different Nature of Convection Over the Maritime Continent and the Tropical Pacific Ocean

The STEP campaign coincided with the January-February monsoon season of the "maritime continent," the region including northern Australia and Indonesia. The STRAT, POLARIS, and ASHOE/MAESA flights are instead over open ocean in the central tropical Pacific, and the convection there is primarily that in the Intertropical Convergence Zone (ITCZ).

The STEP observations include overflights of very deep and violent storms, long-lived tropical cyclones, and some convection over the northern part of the Australian continent [*Russell et al.*, 1993]. Most of the storms overflown during STEP reached altitudes close to the tropopause, whereas ITCZ storms over the ocean rarely do. The maritime continent convection is in general more similar to continental than ocean convection [*Hendon and Woodberry*, 1993]. Hendon and Woodberry examined the properties of convection in tropical regions by using two indicators: (1) deep convective activity (DCA) describing the occurrence only of clouds with $T_b < 230$ K, and (2) IR brightness temperatures (BBT) covering the full range of cloud top temperatures. Over the maritime continent, both DCA and BBT have a pronounced diurnal cycle, and the phase of BBT lags that of DCA by about 3 hours. This relatively short lag is associated with the rapid development of the convection in this region. The DCA develops first with a few small deep convective turrets penetrating to high altitude, while the larger convective complexes take more time to develop and contribute most strongly to the BBT index. Over ocean, the diurnal cycle is relatively very weak. BBT again lags DCA, but over the oceanic ITCZ this lag is 6 hours or longer. The deep convective towers associated with the DCA index are apparently not so closely linked to the development of the larger complexes in this region, or the larger complexes develop more slowly.

This larger lag could in part explain the differences in the correlations between stratosphere gravity wave momentum flux and cloud top temperature seen in Figures 3a and 4d. If the generation of the short horizontal gravity waves is most closely associated with the early formation of the deep convective updrafts, the observations over the ITCZ may simply be missing such events. The STEP observations specifically targeted such deep convection, while the later observations did not. Perhaps the high clouds overflown during STRAT, POLARIS, and ASHOE/MAESA were simply in the late stages of the convective development and did not sample the smaller-scale and more vigorous convective events.

The POLARIS flight on September 23, 1997, may illustrate this possibility. Figure 6 shows the time series of cloud brightness temperature and of the gravity wave momentum flux. Momentum fluxes at times when the aircraft was turning, diving, or climbing have been set to zero as described in section 2.1. The flight path headed due south from Hawaii along the 159.25°W meridian, turned around at 3.37°S latitude, and flew back along the same meridian. Deep convective activity developed to the east of the flight path at about 12°N latitude in the hours before the flight. The ER-2 aircraft flew past this storm on the outbound leg but did not fly directly over the cloud shield; so no signal appears in T_b on the outbound leg. On the return leg, the ER-2 aircraft overflew the cloud, but by this time the storm had dramatically weakened, and no clear signal appears in the momentum flux record (Figure 6b) that

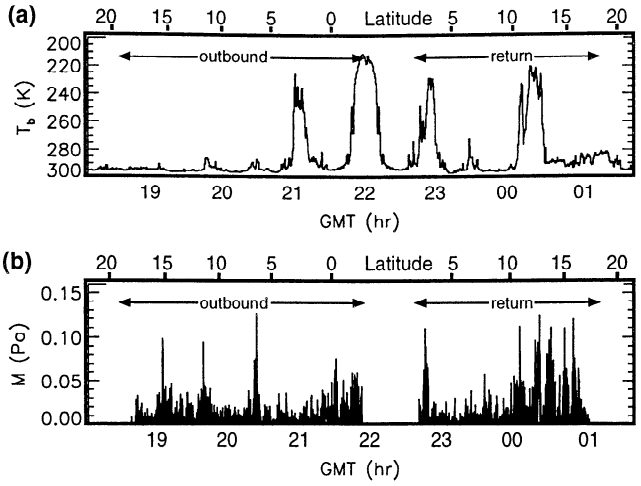

Figure 6. Time series of observations for the POLARIS flight on September 23, 1997. (a) Cloud top brightness temperature below the aircraft. (b) Magnitude of the momentum flux in the stratosphere $\bar{\rho}|u'w', v'w'|$. Aircraft latitude is indicated along the top of the plot.

is well correlated with the cloud temperature (Figure 6a).

It is possible that the STEP observations record larger gravity wave momentum fluxes because the flights (with the exception of flight 5) were designed to investigate aspects of convection directly. Thus large portions of the flight paths were over active deep convection. The ITCZ flights had entirely different objectives; so overflights of high clouds in these data may simply miss the more active phases of the convection. A descriptive summary of the ITCZ flights and associated convection appears in Table 1.

The maximum values in the momentum flux data over the Pacific ITCZ are also significantly smaller than those observed during the STEP campaign (compare Figures 6b and 2a), and similar differences between the STEP observations and those from the other campaigns can be seen on other flights. In general, differences in local maxima in the momentum flux may contribute roughly half of the difference in magnitude at low T_b in Figures 3 and 4.

It is possible that the convection in the ITCZ simply generates much smaller gravity wave momentum flux in the short horizontal wavelength band 5–150 km. The waves generated might alternatively be concentrated in the low-frequency part of the gravity wave spectrum. These waves will have smaller vertical wind amplitudes that might not be detectable by the MMS. Low-frequency waves may also tend to have horizontal wavelengths longer than the necessary 150-km cutoff of the filter used in the present analysis. Lower frequencies can also occur with detectable short horizontal wavelengths of <150 km, but such waves would have shorter vertical wavelengths than their higher frequency counterparts. Shorter vertical wavelengths might be expected for Pacific ITCZ convection because of shallower cloud depth there and associated shallower diabatic heating [*Bergman and Salby*, 1994; *Alexander et al.*, 1995; *Pandya and Alexander*, 1999].

If waves in the Pacific ITCZ data have only moderately lower frequencies than those in the STEP data, they might simply appear at locations further away horizontally from the central source within the cloud, as would be expected from the theory embodied in equation (1). This might confound the one-to-one correspondence between deep clouds and large momentum fluxes.

4. Summary and Conclusions

In situ wind observations in the stratosphere measured by the MMS on the ER-2 aircraft are analyzed to extract information on momentum flux carried by gravity waves with horizontal wavelengths of ~5–150 km. The flux was binned according to the cloud top brightness temperature T_b below the aircraft. The results from the STEP Tropical campaign over Darwin, Australia, in 1987 show a striking relationship between the magnitude of the flux (M) and T_b with largest values $M > 0.11$ Pa over the coldest (highest) clouds $T_b < 240$ K. This relationship between gravity wave and cloud properties results when either onboard infrared radiometer measurements are used or when infrared satellite images are instead used. The flight paths during the STEP campaign were designed to study stratosphere-troposphere exchange processes associated with deep convection and included many overflights of deep active storms.

Collecting flights over convection in the tropical Pacific ITCZ, the relationship between M and T_b is much weaker. Binned momentum fluxes show maximum values of only 0.016 Pa over the deepest clouds with $T_b < 220$ K, approximately 7 times smaller than those observed during STEP. The reasons for the differences are not certain, but several possible factors could be contributing:

1. There could be real differences in the strength of the gravity wave momentum flux above deep convection in the ITCZ and the maritime continent.

2. The relationship between gravity waves and cloud height may be blurred in the ITCZ because of the longer lag between the most active deep convective activity and the development of the larger-scale cloud complex.

3. The STEP observations may observe larger momentum fluxes simply because the flight plans were designed to overfly deep active convection, whereas the ITCZ overflights of convection were coincidental and may not have sampled the most active convection.

4. The ITCZ convection might preferentially generate longer horizontal wavelength waves or waves with low intrinsic frequencies. Such waves cannot typically be observed using these in situ vertical wind measurements. In addition, if waves in the Pacific ITCZ data

have moderately lower frequencies than those in the STEP data, they would appear at locations further horizontally from the central source within the cloud, as would be expected from the theory embodied in equation (1), and this might confound the one-to-one correspondence between deep clouds and large momentum fluxes.

Acknowledgments. This research was supported by the National Science Foundation Physical Meteorology program, grant ATM-989629.

References

Alexander, M. J., and J. R. Holton, A model study of zonal forcing in the equatorial stratosphere by convectively induced gravity waves, *J. Atmos. Sci., 54*, 408-419, 1997.

Alexander, M. J., and L. Pfister, Gravity wave momentum flux in the lower stratosphere over convection, *Geophys. Res. Lett., 22*, 2029-2032, 1995.

Alexander, M. J., and K. H. Rosenlof, Nonstationary gravity wave forcing of the stratospheric zonal mean wind, *J. Geophys. Res., 101*, 23,465-23,474, 1996.

Alexander, M. J., J. R. Holton, and D. R. Durran, The gravity wave response above deep convection in a squall line simulation, *J. Atmos. Sci., 52*, 2212-2226, 1995.

Arkin, P. A., and B. N. Meisner, The relationship between large-scale convective rainfall and cold cloud over the western hemisphere during 1982-1984, *Mon. Weather Rev., 115*, 51-74, 1987.

Bacmeister, J. T., S. D. Eckermann, P. A. Newman, L. Lait, K. R. Chan, M. Loewenstein, M. H. Proffitt, and B. L Gary, Stratospheric horizontal wavenumber spectra of winds, potential temperature, and atmospheric tracers observed by high-altitude aircraft, *J. Geophys. Res., 101*, 9441-9470, 1996.

Bergman, J. W., and M. L. Salby, Equatorial wave activity derived from fluctuations in observed convection, *J. Atmos. Sci., 51*, 3791-3806, 1994.

Chan, K. R., L. Pfister, T. P. Bui, S. W. Bowen, J. Dean-Day, B. L. Gary, D. W. Fahey, K. K. Kelly, C. R. Webster, and R. D. May, A case study of the mountain lee wave event of January 6, 1992, *Geophys. Res. Lett., 20*, 2551-2554, 1993.

Chen, S. S., R. A. Houze Jr., and B. E. Mapes, Multiscale variability of deep convection in relation to large-scale circulation in TOGA COARE, *J. Atmos. Sci., 53*, 1380-1409, 1996.

Dewan, E. M., R. H. Picard, R. R. O'Neil, H. A. Gardiner, J. Gibson, J. D. Mill, E. Richards, M. Kendra, and W. O. Gallery, MSX satellite observations of thunderstorm-generated gravity waves in mid-wave infrared images of the upper stratosphere, *Geophys. Res. Lett., 25*, 939-942, 1998.

Dunkerton, T. J., Theory of the mesopause semiannual oscillation, *J. Atmos. Sci., 39*, 2681-2690, 1982.

Dunkerton, T. J., The role of gravity waves in the quasi-biennial oscillation, *J. Geophys. Res., 102*, 26,053-26,076, 1997.

Fovell, R., D. Durran, and J. R. Holton, Numerical simulations of convectively generated stratospheric gravity waves, *J. Atmos. Sci., 49*, 1427-1442, 1992.

Fritts, D. C., and R. A. Vincent, Mesospheric momentum flux studies at Adelaide, Australia: Observations and a gravity wave-tidal interaction model, *J. Atmos. Sci., 44*, 605-619, 1987.

Hamilton, K., and R. A. Vincent, High-resolution radiosonde data offer new prospects for research, *Eos Trans., AGU, 76*, 497, 506-507, 1995.

Hendon, H. H., and K. Woodberry, The diurnal cycle of tropical convection, *J. Geophys. Res., 98*, 16,623-16,637, 1993.

Holton, J. R., The influence of gravity wave breaking on the general circulation of the middle atmosphere, *J. Atmos. Sci., 40*, 2497-2507, 1983.

Larsen, M. F., W. E. Swartz, and R. F. Woodman, Gravity-wave generation by thunderstorms observed with a vertically-pointing 430 MHZ radar, *Geophys. Res. Lett., 9*, 571-574, 1982.

Lindzen, R. S., Turbulence and stress owing to gravity wave and tidal breakdown, *J. Geophys. Res., 86*, 9707-9714, 1981.

Lindzen, R. S., and J. R. Holton, A theory of the quasi-biennial oscillation, *J. Atmos. Sci., 25*, 1095-1107, 1968.

Liou, K. N., S. C. Ou, Y. Takano, F. P. J. Valero, and T. P. Ackerman, Remote sounding of the tropical cirrus cloud temperature and optical depth using 6.5 and 10.5 mm radiometers during STEP, *J. Appl. Meteorol., 29*, 716-726, 1990.

McLandress, C., M. J. Alexander, and D. L. Wu, Microwave Limb Sounder observations of gravity waves in the stratosphere: A climatology and interpretation, *J. Geophys. Res., 105*, 11,947-11,967, 2000.

Murphy, D. M., Time offsets and power spectra of the ER-2 data set from the 1987 Airborne Antarctic Ozone Experiment, *J. Geophys. Res., 94*, 16,737-16,748, 1989.

Pandya, R. E., and M. J. Alexander, Linear stratospheric gravity waves above convective thermal forcing, *J. Atmos. Sci., 56*, 2434-2446, 1999.

Percival, D. B., and A. T. Walden, *Spectral Analysis for Physical Applications: Multitaper and Conventional Univariate Techniques*, 702 pp., Cambridge Univ. Press, New York, 1993.

Pfister, L., W. Starr, R. Criag, M. Loewenstein, and M. Legg, Small-scale motions observed by aircraft in the tropical lower stratosphere: Evidence for mixing and its relationship to large-scale flows, *J. Atmos. Sci., 43*, 3210-3225, 1986.

Pfister, L., S. Scott, M. Loewenstien, S. Bowen, and M. Legg, Mesoscale disturbances in the tropical stratosphere excited by convection: Observations and effects on the stratospheric momentum budget, *J. Atmos. Sci., 50*, 1058-1075, 1993a.

Pfister, L., K. R. Chan, T. P. Bui, S. Bowen, M. Legg, B. Gary, K. Kelly, M. Proffitt, and W. Starr, Gravity waves generated by a tropical cyclone during the STEP tropical field program: A case study, *J. Geophys. Res., 98*, 8611-8638, 1993b.

Piani, C., D. Durran, M. J. Alexander, and J. R. Holton, A numerical study of three dimensional gravity waves triggered by deep tropical convection, *J. Atmos. Sci.*, in press, 2000.

Ray, E. A., M. J. Alexander, and J. R. Holton, An analysis of the structure and forcing of the equatorial semiannual oscillation in zonal wind, *J. Geophys. Res., 103*, 1759-1774, 1998.

Rottger, J., Structure and dynamics of the stratosphere and mesosphere revealed by VHF radar investigations, *Pure Appl. Geophys., 118*, 494-527, 1980.

Russell, P. B., L. Pfister, and H. B. Selkirk, The tropical experiment of the Stratosphere-Troposphere Exchange Project (STEP): Science objectives, operations, and summary findings, *J. Geophys. Res., 98*, 8563-8589, 1993.

Sato, K., H. Hashiguchi, and S. Fukao, Gravity waves and

turbulence associated with cumulus convection observed with the UHF/VHF clear-air Doppler radars, *J. Geophys. Res., 100*, 7111-7120, 1995.

Scott, S. G., T. P. Bui, K. R. Chan, and S. W. Bowen, The meteorological measurement system on the NASA ER-2 aircraft, *J. Atmos. Oceanic Technol., 7*, 525-540, 1990.

Vincent, R. A., and M. J. Alexander, Gravity waves in the tropical lower stratosphere: An observational study of seasonal and interannual variability, *J. Geophys. Res., 105*, 17,971-17,982, 2000.

Zhang, C., On the annual cycle in the highest, coldest clouds in the tropics, *J. Clim., 6*, 1987-1990, 1993.

M. J. Alexander, Colorado Research Associates, a Div. of NorthWest Research Associates, 3380 Mitchell Lane, Boulder, CO 80301. (alexand@colorado-research.com)

J. H. Beres, Atmospheric Science, University of Washington, Box 351640, Seattle, WA 98195-1640. (beres@atmos.washington.edu)

L. Pfister, NASA Ames Research Center, Moffett Field, CA 94035-1000. (pfister@telsci.arc.nasa.gov)

(Received November 5, 1999; revised May 11, 2000; accepted May 16, 2000.)